Environmental Science & Technology

ARTICLE

pubs.acs.org/est

Composition of Smoke Generated by Landing Aircraft

Michael Bennett,*[,†] Simon M. Christie,[†] Angus Graham,[†] Bryony S. Thomas,[†] Vladimir Vishnyakov,[†] Kevin Morris,[‡] Daniel M. Peters,[§] Rhys Jones,[§] and Cathy Ansell[§]

[†]Centre for Aviation, Transport and the Environment, School of Science and the Environment, Manchester Metropolitan University, Chester Street, Manchester M1 5GD, U.K.

[‡]British Airways PLC, Waterside (HBA3), P.O. Box 365, Harmondsworth UB7 0GB, U.K.

[§]Atmospheric, Oceanic and Planetary Physics, Clarendon Laboratory, University of Oxford, Parks Road, Oxford OX1 3PU, U.K.

ABSTRACT: A combination of techniques has been used to examine the composition of smoke generated by landing aircraft. A sample of dust from the undercarriage from several commercial airliners was examined with SEM/EDX (Scanning Electron Microscope/Energy Dispersive X-ray) to determine its elemental composition and also with an aerosizer/aerodisperser in order to measure the particle size spectrum. The observed size spectrum was bimodal with equal numbers of particles at peaks of aerodynamic diameter ~10 μm and ~50 μm. The EDX analysis suggested that the former peak is carbonaceous, while the latter consists of elements typical of an asphalt concrete runway. In the field, a scanning Lidar, in combination with optical and condensation particle counters, was deployed to obtain limits to the number concentration and size of such particles. Most of the (strong) Lidar signal probably arose from the coarser 50 μm aerosol, while respirable aerosol was too sparse to be detected by the optical particle counters.

INTRODUCTION

Local air quality is one of several issues constraining the development of airports. In Europe, the most pressing of such limits is that related to the legally enforceable limit on the long-term average of NO_2, e.g. at Heathrow.[1] Strategically, however, one might be more concerned by local concentrations of respirable particulate. While concentrations of fine particulate matter (PM) in the Heathrow area lie comfortably within the proposed long-term limit for $PM_{2.5}$ of 25 μg m^{-3}, there is apparently no safe threshold for such PM, with even very modest variations in fine urban aerosol having an epidemiologically detectable effect on mortality.[2]

Conventionally, most of the modeling of the impact of commercial aviation on PM concentrations has concentrated on emissions from aero-engines. This is despite the smoke emitted from aircraft on landing being clearly visible to the naked eye, while that from modern aero-engines on full power is scarcely visible. When an aircraft lands, the main wheels make contact with the ground and spin up; the nose wheel drops to the ground; the brakes are then applied to bring the aircraft to a halt. Visible smoke is usually only released only as the wheels spin up, though the brakes must subsequently release fine aerosol as they abrade. Integrated over the landing and takeoff (LTO) cycle, it is not clear what should be the largest source of respirable aerosol.

From mass balance calculations,[3,4] we know that the rubber lost per landing is very large (anything up to ~1 kg from a B747). We know — both from the odor and from recent measurements [5] of organic carbon and associated trace metals in nearby ambient PM — that some must be emitted as fine aerosol, but we do not know how much of this is so dispersed and how much adheres to the runway or is scattered as macroscopic fragments. By contrast, recent estimates using the best available understanding of PM emissions from aircraft engines, including nonvolatiles, sulfates, and volatile organics,[6] suggest that total engine emissions are somewhat smaller (anything up to ~0.25 kg of PM per LTO cycle from a B747 with four RB211−524G power plant), though in this case all of the emissions are initially released as fine aerosol.[7] Furthermore, while PM emission integrated over the LTO cycle may be a useful metric in the development of airport emissions inventories, it may not be the best metric for airport air quality applications, since here it is the ground level emissions that dominate. Thus, brake and tire wear were estimated to be the dominant source of PM at Gatwick, accounting for 69% of the total ground-level PM_{10} emissions from aircraft.[8] Overall, however, this contribution is subject to significant uncertainty: PM emissions from tires and brakes are dependent on many factors including aircraft weight, speed, number of wheels, brake material (carbon or steel), weather conditions, undercarriage design, pilot actions, and airline procedures.

Received: August 12, 2010
Accepted: March 15, 2011
Revised: February 10, 2011
Published: March 24, 2011

dx.doi.org/10.1021/es1027585 | *Environ. Sci. Technol.* 2011, 45, 3533–3538

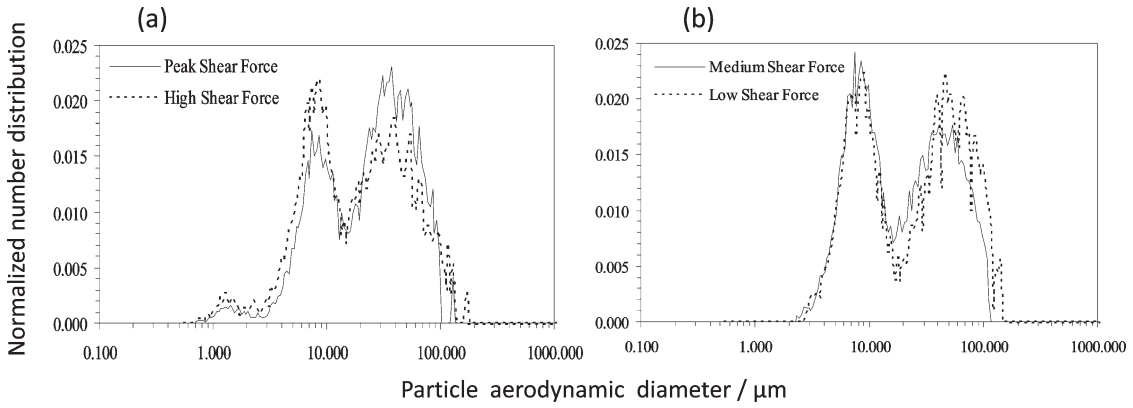

Figure 1. Particle size spectrum of sample of dust on landing gear measured with an Aerosizer and an Aerodisperser employing (a) high and (b) low shear.

The proportion of the mass loss from aircraft tires and brakes that becomes suspended as fine PM has not been extensively studied. For road vehicles it is generally estimated that less than 10% of tire loss is emitted at PM_{10} - though the proportion could be as high as 30%.[9] Within this, the larger particles may be generated through mechanical abrasion, while the submicrometer fraction may arise from the thermal degradation of tire polymer and the volatilization of extender oils.[10] For road vehicle brake wear, on the other hand, ref 11 observed that between 50% and 90% of brake emissions are emitted as airborne PM with a number weighted mean aerodynamic diameter of 1−2 μm. Similarly, a study described in ref 12 estimated that 70% of the eroded material from road vehicle brakes ends up as airborne PM.

For estimating the PM_{10} emissions from aircraft tires and brakes, the Project for the Sustainable Development of Heathrow[1] used upper limits of 10% for tire wear and 100% for brake wear. These limits were chosen to reflect the fact that braking conditions for aircraft are considerably more aggressive than those for road vehicles in normal use. It was also assumed that PM emissions scale linearly with the weight of the aircraft. Such estimates, however, remain speculative.

To tighten the upper emission limits of respirable aerosol in tire smoke, we report here a field trial of Lidar measurements with simultaneous point observations of tire smoke, together with SEM and size spectrum analyses of dust collected from aircrafts' undercarriage.

In the past few years, Lidar has become the technique of choice for examining the dispersion of material in aircraft exhaust plumes.[13−16] The principal limitation of the method is that the observed signal strength depends on the size spectrum of the scattering particles and on their refractive index. If neither is known, a simple backscatter Lidar is normally limited to measuring advection and dispersion rather than absolute concentrations. In the case of this study, however, we have additional information arising from laboratory analyses of undercarriage dust, which we presume to be representative of the coarser fraction of landing-generated smoke. This has enabled us to make gravimetric estimates of the quantity of coarse dust which must have been present to generate the observed Lidar signal. In addition the deployment of optical particle counters (OPCs) within the Lidar scanning plane allows us to put an upper limit on fine particle concentrations within the plume.

Size Spectrum of Undercarriage Dust. We analyzed a composite sample of 909 mg of landing and braking dust collected from the undercarriage (oleo legs) and wheel hubs of three Airbus A320−232 aircraft of the BA fleet, parked on the stands at Heathrow. The sample was greyish-black, consistent with its containing a high proportion of black carbon. It was dry, containing no visible lubricant. The dust was simply collected with a paint brush into a sealed jar.

Such a sample must have contained PM from a variety of sources (tires, brakes, runway, taxiways, etc.). Not having the analytical tools to predict with any confidence which might be preferentially deposited where, however, we considered that a well-mixed composite sample was most appropriate. Conversely, the aircraft landing gear would be extremely inefficient in collecting respirable aerosol. Coarse aerosol will thus be over-represented in the sample. We may note that all the runways at Heathrow are of grooved asphalt, while apron surfaces are concrete. Brakes are carbon−carbon.

A second sample was collected from a B757−236 and a B747−436 aircraft. During collection it was noted that the amount of dust adhering to these aircraft appeared to be much greater than those of the A320s. This presumably happens since the Boeing bogies are mounted fore-and-aft; the aft undercarriage and wheel can thus collect the aerosol generated by the forward wheel.

The size spectrum of dust from the A320s was determined using an Aerosizer instrument which determines the aerodynamic diameter of PM through time-of-flight measurements.[17] It does so by accelerating the particles in a supersonic flow and then measuring their velocity. The instrument was calibrated with NIST-traceable polystyrene latex spheres. It has a lower size cutoff at an aerodynamic diameter of ~0.5 μm.

An Aerodisperser was used to transfer the dust sample into the instrument. It consists of a polished stainless steel spherical cup into which the powder sample is placed. High pressure air from a small nozzle is pulsed into the cup and any entrained dust is then transferred to the Aerosizer sample line. The duty cycle (though not the pressure) of the pulses is gradually increased to 100%, by which point the entire sample has been used up: none remains in the cup. The sample is then passed through an aperture into the optical sizing chamber. Adjusting the diameter of the aperture adjusts the shear experienced by the particles: this may lead to aerosol deagglomeration.[18]

The dust sample size distribution was measured using a range of aperture settings, with the results shown in Figure 1. As may be seen, the distribution is bimodal, with peaks at aerodynamic

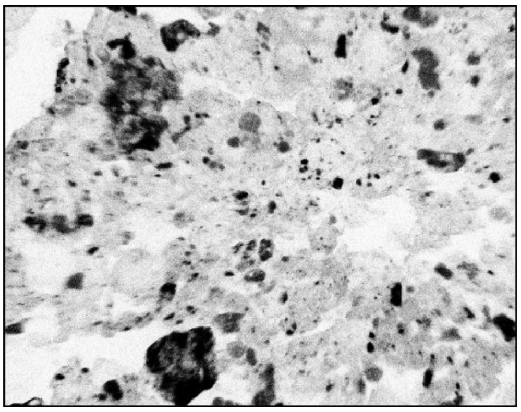

Figure 2. EDX image of Si in undercarriage dust. Frame width is 380 μm.

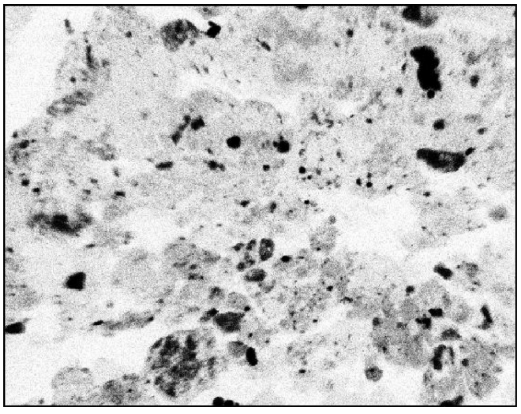

Figure 3. EDX image of Al in undercarriage dust. Frame width is 380 μm.

diameters of about 10 and 50 μm. (Clearly, because of the very poor collection efficiency for respirable aerosol, the plotted size spectrum for aerodynamic diameters <10 μm should be taken as a lower limit to the relative number density of particles originally present.)

It is interesting to note that an additional small peak of fine aerosol (1−2 μm) is seen at the highest shear settings. Had the captured dust originally been generated by a high shear event (e.g., between tires and runway) we should not have expected the shear in the Aerodisperser to break up the dust further. The measured size spectrum should then be more or less independent of the shear setting − as we see for the peaks at 10 and 50 μm. On the other hand, soot agglomerations (e.g., from burning rubber) are relatively fragile and may be broken up by the higher shear settings in the Aerodisperser. The 1−2 μm peak may indicate the occurrence of such a process.

SEM Measurements. The dust sample was also analyzed at the John Dalton Institute in MMU using a Zeiss Supra 40VP SEM. Besides electron backscatter analysis, this system can perform EDX for identification of the elemental composition of particles and micro-Raman for measurements of chemical composition. (The latter was not employed in the present study.)

A uniform layer of dust was prepared for analysis by placing an adhesive carbon disk into the bulk sample. Our standard analyses of each sample included images of backscattered and secondary electrons (the latter being more sensitive to surface topography)

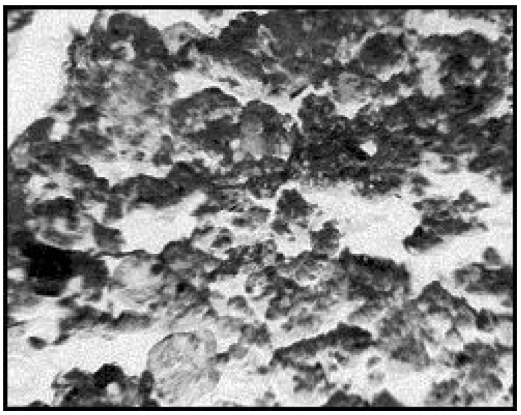

Figure 4. EDX image of C in undercarriage dust. Frame width is 380 μm.

and EDX. X-ray spectral peaks integrated over the observation area were mapped for Al, Ca, C, Cl, Co, Cr, Cu, Fe, K, Mg, Mn, Na, Ni, O, P, Si, S, Ti, V, and Zn. A selection of these maps is shown in Figures 2-5.

Figure 2 shows the Si distribution in the sample. This element may be taken as a general marker of dust lifted mechanically from the ground surface (though it should be noted that precipitated synthetic silica is also added to tire treads to improve wet traction). Particle sizes in the image range from 1 μm (the spatial resolution of the map) up to 63 μm. By correlating the elemental compositions of these particles, an attempt at identification of various minerals may be made. Thus, the large dark particle at the bottom of the image is only evident in Si and O: we may interpret it as quartz, a component of many rocks (or of concrete: elsewhere in the image, there are many particles containing Ca). Conversely a particle in the top right corner of the image is also associated with Al (Figure 3), K, and O. It may be a type of feldspar which is, along with quartz, a component of granite. Aluminum hydroxide is also included in some tire formulations to enhance wet grip performance and abrasion resistance.

All of these mineral particles appear to be embedded in a carbonaceous substrate (Figure 4). At this stage, this substrate no longer showed any very clear structure; soot aggregates have little mechanical strength. We thus have little indication of the provenance or initial size structure of the carbonaceous aerosol. Soot may arise from the burning of the tire rubber, or of the tar binding an asphalt concrete runway, or from abrasion of the brakes. Carbon black is, of course, a major component of tires, and carbonaceous aerosol would be generated on landing even in the absence of combustion. Some indication of the source may be given by the presence of other trace elements, e.g. S or Zn. S is used as a vulcanizing agent in rubber and will also be present in tar. The EDX images did indeed show a weak background of S, associated with the C signal, consistent with the soot arising from one of these sources. There were also some 1 μm particles of S, a few of which were associated with Ca (i.e., gypsum), while others gave a strong signal on the backscattered SEM signal but not from any of the other cations which we measured, nor from O. They may have been particles of MoS_2, which is commonly used as a lubricant in aero-engines.

Zn is used as an adjunct to S in vulcanizing rubber, while Cr may also be present in tires.[19] A few 1 μm particles of Cr/Zn were indeed detected, though not associated with S. If these particles originated from burning rubber, the implication is that the S

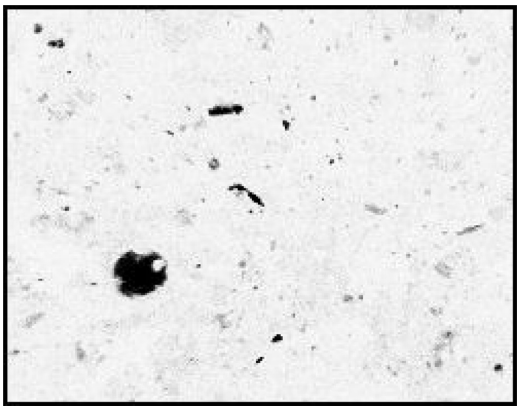

Figure 5. EDX image of Fe in undercarriage dust. Frame width is 380 μm.

Figure 6. FAAM aircraft taxiing to takeoff at Cranfield, 17/2/09. The inputs to the Grimm samplers are on the stand to the right of the photograph. The Lidar is 375 m to the right of the frame; it was aligned on the Osiris, which is the instrument standing in the center of the photograph.

compounds also generated were sufficiently volatile to be separated from more refractory products of combustion.

In Figure 5, we can see a small (35 μm) droplet of Fe, associated with Co and traces of Mn, Ni, V, and Zn. We note that it is quite common to find droplets of iron of diameter mm in asphalt concrete — this is presumably the extension of the size spectrum down to the microscopic scale. Figure 5 also shows some irregularly shaped Fe PM at diameters of 10 μm or below. The provenance of these is not obvious.

Field Measurements. A field trial was made at Cranfield Airport (52° 4.33′ N, 0° 37.00′ E) on 17 February 2009. Instruments available were (among others) a Rapid-Scanning Lidar,[15] a condensation particle counter (Grimm UPC), and two OPCs (Grimm 1.108; Turnkey Instruments Osiris) (Figure 6). In addition, video recordings of all operations were taken with a video camera from the control tower. An instrumented BAe146 aircraft (www.faam.ac.uk) made eight sorties, each consisting of a takeoff, circuit, and landing. On the final sortie, the pilot was requested to make a heavy landing (the final descent speed of the aircraft was 2.0 m s^{-1} as against a more typical value of 0.4 m s^{-1}), and it is measurements of the smoke from this landing that

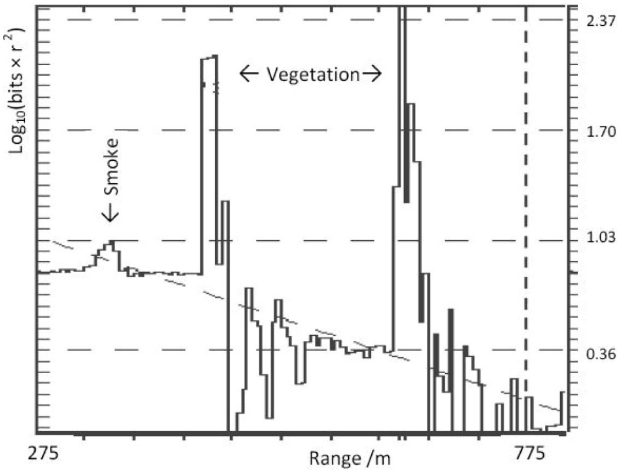

Figure 7. Lidar return at low elevation through tire smoke. The graph shows the logarithm of signal as a function of range, corrected for geometric spreading. The dashed line is an attempt to fit the backscatter arising from the ambient aerosol: in this case the algorithm has been confused by hard returns at 450 and 650 m, making manual analysis necessary.

we will present here. The BAe146 has two pairs of landing wheels, each with Goodyear 393F-53-1 tires.

The runway at Cranfield is aligned 212°-32° (true); there is a preference to land and take off toward the SW. The Lidar was set up near the N end of the airfield and for the monitoring of tire smoke scanned vertically on an azimuth of 175.7° (true), crossing the runway centerline at a range of 252 m.

There was a moderate NW cross-wind on the day of the trial, advecting both engine and tire smoke emissions away from the Lidar. The point samplers were deployed on the airfield close to the Lidar's scanning plane and at a distance of 123 m beyond the runway centerline. At this position, burning rubber could be smelled on all landings and kerosene on most of the taxiing out and take-offs (hydrocarbon emissions are greater at lower power settings).

The Grimm UPC easily detected the emissions from the aircraft on taxiing, takeoff, and landing, with typical peak number concentrations being respectively 7×10^5 cm^{-3}, 4×10^5 cm^{-3}, and 1×10^5 cm^{-3}. On landing, the aerosol peak was usually bifurcated, presumably by the wing vortices. (On takeoff, the aircraft would not yet have been moving fast enough at the measuring point to generate significant lift: at the point of landing, by contrast, it flairs and would have been generating slightly more lift than its weight.) We note that although the fuel burn while taxiing was only 13% of that in the takeoff run, the aircraft was moving an order of magnitude more slowly. This is all fine PM, since the 50% cutoff point for the sampling line was at an aerodynamic diameter of about 3 μm. The number density of coarser PM should in any case be negligible by comparison.

The Lidar was also capable of detecting the engine plume on takeoff and the tire smoke on landing −6 out of the 8 landings were so detected. The Lidar signal comes from outgoing radiation backscattered by atmospheric aerosol. This is normally expressed through a parameter, β, being the proportion backscattered per unit path length per unit solid angle. Inevitably, this is associated with an extinction, α, which is the fraction of radiation lost per unit path length. A log−linear plot of signal against range in uniformly hazy air will thus appear as a straight line of slope -2α.

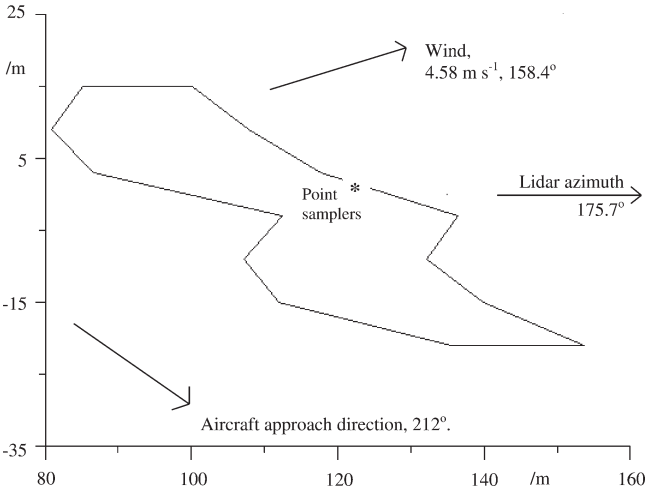

Figure 8. Footprint of tire smoke at 4.1 m above the surface in relation to point samplers at 14:15:31 UTC. For convenience, coordinates are relative to the Lidar scanning azimuth, with an origin where this crosses the runway centerline. Directions are given in degrees from true North.

Figure 7 shows a backscatter profile from a single shot at close to ground level shortly after the aircraft had landed. The strong returns at ranges of 450 and 650 m are from vegetation and may be ignored. The small backscatter peak at 350 m is the tire smoke, which has not yet reached the point samplers, which were at 375 m. In the following scan, 4 s later, the smoke puff had almost passed the point samplers. The peak backscatter of the smoke in Figure 7 corresponds to an excess backscatter of 58% relative to the ambient backscatter; in the following scan, it was 48%. (The method of calculation is described in ref 16). From ref 20, we know that for a Lidar wavelength of λ = 355 nm in humid marine aerosol, the ambient extinction/backscatter ratio, α/β, should be ~24 sr. Taking the average of several neighboring low-elevation shots, away from tire smoke or ground clutter, the ambient extinction was found to be $\alpha = 2.25 \times 10^{-4}$ m^{-1}. By implication, the peak excess backscatter when the puff passed over the samplers should be $\beta \sim 0.50 \times 10^{-5}$ m^{-1} sr^{-1}.

Suppose that the puff consists of spheres of number density n, diameter $d = 2r \gg \lambda$, albedo a and density ρ, and that incident light is backscattered over 2π sr. Simple geometry then tells us that the backscatter should be $\beta = ar^2n/2$. Rearranging, we see that $n = 2\beta/(ar^2)$. Likewise, the gravimetric concentration should be $\chi = 8\pi\rho r\beta/(3a)$. Sections 3 and 4 suggest that the particles could be represented as aged concrete ($a \sim 0.25$, $\rho = 2400$ kg m^{-3}) of diameter ~50 μm. Hence, peak concentrations within the plume should be $n \sim 64$ L^{-1} and $\chi \sim 50$ mg m^{-3}. The supplementary peak in PM at aerodynamic diameters of ~10 μm is likely to contribute very little to the backscatter since, as may be seen from Figure 1, its peak number density is comparable to that of the larger particles.

Even for such coarse particles, the Stokes fall velocity is <0.2 m s^{-1}, so sedimentation is initially secondary to the gross flow and turbulence within the emission. Over the 27 s for which it was observed, the center-of-gravity of the puff did not fall but rose by 3.5 m.

Figure 8 shows the implied footprint of the tire smoke at a height of ~4 m and at the time when it is passing over the point samplers. For this analysis we have used the 10 m wind speed and direction observed at the Lidar to shift the envelope of tire smoke observed in earlier or later scans to that at the reference time. We can see that the smoke extends 75 m along the line of the runway. For a landing speed of 57.1 m s^{-1}, this implies a total smoke emission time of 1.3 s. This is much longer than the time for which visible smoke was generated, the video footage showing that this lasted for 0.32 s at most, with the main wheels landing essentially simultaneously. The Lidar is of course much more sensitive than the eye. Part of the greater longitudinal extension of the smoke may possibly arise from some PM being entrained in the wake of the aircraft.

Although the Lidar signal is dominated by the largest particles, these would be barely observable by the point samplers, since they would be aerodynamically too massive to pass though the sample line. (The 50% capture point of the system is at an aerodynamic diameter of about 8 μm.) On the other hand, the measured size spectrum (Figure 1) suggests that the number density at $d = 10$ μm is at least comparable with that at $d = 50$ μm: given the poor capture efficiency of respirable PM by the structure of the aircraft, there may in fact be many more fine particles than coarse particles emitted. If so, we should have been able to detect the larger particles with the Lidar and the smaller particles with the OPCs. The volumetric sampling rates of the Osiris and the Grimm 1.108 were 0.6 L min^{-1} and 1.2 L min^{-1}, respectively, each with a 1 s sampling time, so over the ~5 s period for the puff to pass they should have provided number sensitivities of ~20 L^{-1} and ~10 L^{-1}, respectively. In practice, however, the sensitivity was determined by the background noise. Thus, for the Osiris, the observed background signal levels were 32 ± 16 μg m^{-3} for PM_{10}, 10 ± 2 μg m^{-3} for $PM_{2.5}$, and 3 ± 0.5 μg m^{-3} for $PM_{1.0}$, corresponding to respective number densities of 41 L^{-1}, 815 L^{-1}, and 3820 L^{-1} for spheres at the top end of these size ranges. PM_{10} in the tire smoke should thus have been at or above the practical detection limit of this instrument. In fact, nothing significant was seen with either instrument in any size range, implying that Figure 1 has not grossly underestimated the number density at 10 μm. It is clear that the visible smoke cannot be associated with a substantial emission of respirable PM.

The ultrafine plume measured with the Grimm UPC arrived at the sampling point simultaneously with the tire smoke. Unlike the tire smoke, however, it persisted for 40 s. As after other landings, this ultrafine plume (i.e., engine smoke) was double-peaked, with a peak number concentrations of successively 1.1×10^5 mL^{-1} and 1.3×10^5 mL^{-1}. Almost nothing of the secondary peak, however, was visible with the Lidar. It is interesting that almost all of the tire smoke should apparently have been entrained into the port wing vortex.

Reference 4 estimated that the rubber lost per aircraft landing amounts to a fraction 2×10^{-6} of the maximum takeoff weight of the aircraft. For the FAAM aircraft, this comes to 74 g. Integrating over all shots in Figure 8 for which smoke was visible, and multiplying by the estimated lateral displacement (6.0 m) between scans, we obtain a total mass of visible smoke within the puff of 24 g (taken as 50 μm concrete particles). The implication of Figure 1 is that these coarser particles comprise ~200× as much mass as the 10 μm peak. The clear implication is that only a tiny proportion of the rubber lost can be as respirable aerosol: the great majority must remain on the runway surface.

DISCUSSION

The differing sensitivities of the various monitoring methods in these trials is quite striking. At the target distance in this trial, the Lidar had a sampling volume of ~550 L. It was thus sensitive to the sparse, coarse aerosol generated by the landing aircraft. The point samplers struggle to resolve this, not merely because of

the poor statistics of a particle happening to be within the sampled volume (10−20 mL s^{-1}) but also because dynamical constraints make coarse aerosol unlikely to pass along the sampling line. Jointly, these observations suggest that the bulk of the visible aerosol in tire smoke is too coarse to be respirable: it seems to consist largely of mechanically generated dust from the runway surface. Mass balance considerations imply that very little of the tire rubber lost is released as fine aerosol.

The condensation particle counter (Grimm UPC), on the other hand, is extremely sensitive to ultrafine particles. While it detected the engine emissions very sensitively, there were simply far too few particles in the tire smoke to provide a distinguishable signal.

Overall, it would appear that while tire smoke emissions can be spectacular, and may have operational implications in terms of tire wear and runway degradation, the emission of respirable PM is relatively modest. There may, however, still be health issues arising from hazardous organics (e.g., PAHs) volatalized from the rubber or of nuisance from the associated odor.

AUTHOR INFORMATION

Corresponding Author

*E-mail: m.bennett@mmu.ac.uk.

ACKNOWLEDGMENT

The field measurements at Cranfield were funded by the Omega Consortium. We thank the management and staff of FAAM and Cranfield airport for their generous assistance in these trials and also Richard Hill of Westlakes Scientific Consultancy Ltd. for many valuable discussions.

REFERENCES

(1) UK Department for Transport. *Project for the Sustainable Development of Heathrow, Annex 1*. 2006. www.dft.gov.uk/pgr/aviation/environmentalissues/heathrowsustain/ (accessed March 21, 2011).

(2) Environmental Protection Agency. *Provisional Assessment of Recent Studies on Health Effects of Particulate Matter Exposure*. EPA/600/R-06/063; July 2006. www.epa.gov/pm/pdfs/ord_report_20060720.pdf (accessed March 21, 2011).

(3) Curran, R. *Method for estimating particulate emissions from aircraft brakes and tyres*. QINETIQ/05/01827; Farnborough, UK; 2005. www.dft.gov.uk/adobepdf/165217/282786/8_Brakes_TyresIssue3.pdf (accessed March 21, 2011).

(4) Morris, K. (2006) *An estimation of the tyre material erosion from measurements of aircraft tyre wear*. British Airways Environmental Affairs, ENV/KMM/1131/14.18; 2006. http://britishairways.it/cms/global/pdfs/csr/PSDH_Technical_Reports.pdf (accessed March 21, 2011).

(5) Amato, F.; Moreno, T.; Pandolfo, M.; Querol, X.; Alastuey, A.; Delgado, A.; Pedrero, M.; Cots, N. Concentrations, sources and geochemistry of airborne particulate matter at a major European airport. *J. Environ. Monit.* **2010**, *12*, 854–862.

(6) Hurley, C. D.; Eyers, C. J.; Calvert, W. J. *Estimation of total particulate emissions from civil aero engines at London Heathrow*. QINETIQ/06/00472, Farnborough, UK; 2006. http://www.dft.gov.uk/adobepdf/165217/282786/9_Particulates-Final.pdf (accessed March 21, 2011).

(7) Intergovernmental Panel on Climate Change. *Aviation and the global atmosphere, Chapter 3*. 2000. www.grida.no/publications/other/ipcc_sr/ (accessed March 21, 2011).

(8) BAA. *Gatwick Emissions Inventory 2002/2003*; 2006. http://www.gatwickairport.com/Documents/business_and_community/Publications/2006/Emission_inventory2002_03.pdf (accessed March 21, 2011).

(9) Boulter, P. G. *A review of emission factors and models for road vehicle non-exhaust particulate matter*. PPR065, Environmental health & risk management; Univ. of Birmingham, UK; 2005. http://www.air-quality.co.uk/reports/cat15/0706061624_Report1__Review_of_Emission_Factors.PDF (accessed March 21, 2011).

(10) Cadle, S. H.; Williams, R. L. Gas and particle emissions from automobile tyres in laboratory and field studies. *Rubber Chem. Technol.* **1978**, *52*, 146–158.

(11) Sanders, P.; Ning, Xu; Dalka, T.; Maricq, M. Airborne brake wear debris: size distribution, composition and a comparison of dynamometer and vehicle tests. *Environ. Sci. Technol.* **2003**, *37*, 4060–4069.

(12) UNECE *Automobile brake and tyre wear*. 2003. http://vergina.eng.auth.gr/mech/lat/PM10 (accessed March 21, 2011).

(13) Wayson, R.; Fleming, G.; Kim, B.; Eberhard, W.; Brewer, W. *Final report: the use of LIDAR to characterize aircraft initial plume characteristics*; US Dept Trans, FAA; 2004. www.volpe.dot.gov/air/docs/2004-dts-34-fa34t-lr3.pdf (accessed March 21, 2011).

(14) Christie, S.; Bennett, M.; Graham, A.; Raper, D. W. Lidar monitoring of aircraft emissions for environmental air quality. *Photon 06*, 4−7 September, 2006, Manchester, UK. http://photon06archive.iop-confs.org/Optical%20environmental%20sensing%20I%20Wed%2010.45.doc (accessed March 21, 2011).

(15) Bennett, M.; Christie, S. An application of backscatter Lidar to model the odour nuisance arising from aircraft tyre smoke. *Int. J. Environ. Pollut.* **2011**, *44*, 316–328.

(16) Bennett, M.; Christie, S.; Graham, A.; Raper, D. W. Lidar observations of aircraft exhaust plumes. *J. Atmos. Oceanic Technol.* **2010**, *10*, 1638-1651. DOI: 10.1175/2010JTECHA1412.1.

(17) Chuen, J. T.; Hung, M. C.; Shu, T. C.; Jong, Y. K. Performance evaluation of an API Aerosizer. *J. Aerosol Sci.* **1998**, *29*, 839–853.

(18) Safatov, A. S.; Yashin Kulkin, S. N.; Frolov, V. G.; Shishkin, A. V.; Buryak, G. A. Variations in disperse composition of dry powders according to energy of their dispersion. *Powder Technol.* **1998**, *97*, 227–232.

(19) Ma, C.-J.; Tohno, S.; Kasahara, M. A case study of the single and size-resolved particles in roadway tunnel in Seoul, Korea. *Atmos. Environ.* **2004**, *38*, 6673–6677.

(20) Ackermann, J. The extinction-to-backscatter ratio of tropospheric aerosol: a numerical study. *J. Atmos. Oceanic Technol.* **1998**, *15*, 1043–1050.